Available online at www.sciencedirect.com
ScienceDirect
Geochimica et Cosmochimica Acta 70 (2006) 4181–4195
Geochimica
www.elsevier.com/locate/gca

Modeling of smectite illitization in burial diagenesis environments

Javier Cuadros *

Department of Mineralogy, Natural History Museum, Cromwell Road, London SW7 5BD, UK

Received 8 March 2006; accepted in revised form 19 June 2006

Abstract

The kinetics of smectite illitization in shale samples from eight wells have been modeled using the equation $-dS/dt = kK^{0.25}S^5$ [Cuadros, J., Linares J., 1996. Experimental kinetic study of the smectite-to-illite transformation. *Geochim. Cosmochim. Acta* **60**, 439–453], where S is the proportion of smectite layers in illite-smectite (I–S), t is time, k is the rate constant and K is the concentration of potassium. The I–S compositions and the physical parameters were obtained from the literature. Potassium concentration is the only unknown parameter and it was chosen to fit the experimental data. I propose that this variable is termed "effective K concentration," as it is affected not by the actual K concentration alone but also by those of other cations that compete with K for the smectite interlayer sites, especially Ca, by ion mobility in the sediments and possibly by other variables. The kinetic equation allows an accurate fit to the experimental data in all the wells, reproducing both the illitization onset and the patterns of the plots of % smectite vs. depth. The relative changes of the values of "effective K concentration" compare well with K/Ca equivalent ratios in the whole rock. Three of the modeled wells, located in near proximity, produced similar "effective K concentration" patterns. These results support the validity of the equation used in the models. They also suggest that this equation can be used to assess K concentrations in sediments and K mobility within basins.

1. Introduction

Smectite illitization is an important reaction in burial diagenesis as it influences greatly the chemical and physical evolution of the sediments by controlling sediment porosity, water release and overpressure and affecting the chemical budget of elements such as Si, Ca, Na and K. Smectite and smectite illitization have also been linked to oil formation and migration, respectively (e.g., Perry and Hower, 1972; Hower et al., 1976 and references therein). The reaction has been modeled by several authors using field samples and laboratory experiments to produce kinetic equations. Some of these equations have been tested against the progress of the reaction in sedimentary basins where the several variables could be reasonably constrained (Pytte and Reynolds, 1989; Elliott et al., 1991; Velde and Vasseur, 1992; Huang et al., 1993; Hillier et al., 1995; Elliott and Matisoff, 1996; Elliott et al., 1999), with the result that none of the kinetic equations has been found to be consistently superior to the others. Hence, the search for the equation governing the rate of smectite illitization is still open. In this paper, I (1) discuss the choice of the type of equation for modeling purposes, (2) discuss the meaning of the K concentration variable and (3) use the equation obtained by Cuadros and Linares (1996) in their experimental study to model the progress of the illitization reaction in several basins.

2. Type of kinetic equation

The smectite-to-illite reaction can be written in a simplified way as $[Si_4]^{tet}\ [Al_{1.8}Mg_{0.2}]^{oct}\ (Ca, Mg, Na)_{0.2}\ O_{10}(OH)_2 + K \rightarrow [Si_{3.4}Al_{0.6}]^{tet}\ \ [Al_{1.8}Mg_{0.2}]^{oct}\ \ K_{0.8}O_{10}(OH)_2 +$ Silica + Ca + Mg + Na, where tet and oct refer to the composition of the tetrahedral and octahedral sheets. The formulas in the equation are idealized and are intended only to show the main features of the chemical transformation. There is no attempt to balance the equation as there is no agreement about several details in it. For example, the relative increase in Al content in illite can be due both to silica loss and to Al input. The essential facts are that the

* Fax: +20 7942 5537.
E-mail address: j.cuadros@nhm.ac.uk.

0016-7037/$ - see front matter © 2006 Elsevier Inc. All rights reserved.
doi:10.1016/j.gca.2006.06.1372

layer charge increases mainly through Al for Si substitution in the tetrahedral sheet and that the originally exchangeable cations (Ca, Mg, Na are the most common) are substituted by K. The illitization reaction occurs via the mixed-layer I–S.

Data from sedimentary basins where the complete smectite-to-illite transformation has been recorded show typical "Z-shaped" plots of % smectite vs. depth (Fig. 1, dash-line curve). In these plots, the proportion of smectite in I–S decreases little with depth in the shallow sediments, then it decreases abruptly up to a value that has frequently found to be ~20%, and finally it decreases slightly or remains constant in the deeper sediments. These three steps in the sequence of illitization have been frequently recognized. The first step is evidently due to the fact that the temperature of the sediments is low and thus the illitization reaction has not started yet or is still very slow. In the second step, the temperature reaches values at which the illitization reaction is sufficiently fast and produces a rapid reduction of the smectite proportion. Some authors have proposed explanations for the change of the slope from the second to the third step invoking changes in the variables controlling the transformation (especially K availability) or in the illitization process itself. However, the Z-shape of these plots is modeled without having recourse to such changes, when using a kinetic equation of the type $-\mathrm{d}S/\mathrm{d}t = kK^mS^n$, where S is the proportion of smectite layers in I–S, t is time, k is the rate constant and K is the concentration of potassium. The solid-line curve in Fig. 1 is calculated using such a type of equation, for constant K and a constant rate of temperature increase (i.e., constant sedimentation rate and geothermal gradient). At this point, I will only discuss the equation in general terms; I will give details of the calculations later. If the exponent n used in the equation is higher than one, the reaction rate becomes increasingly dependent on S, the more so as the value of n is higher. At the beginning of the reaction, when S is close to one, n does not greatly affect the reaction rate, but when S becomes smaller as the reaction proceeds, increasing the value of n has a great effect in slowing down the reaction. This means that large n values cause large changes in the slope of the % smectite vs. depth plots (second to third step).

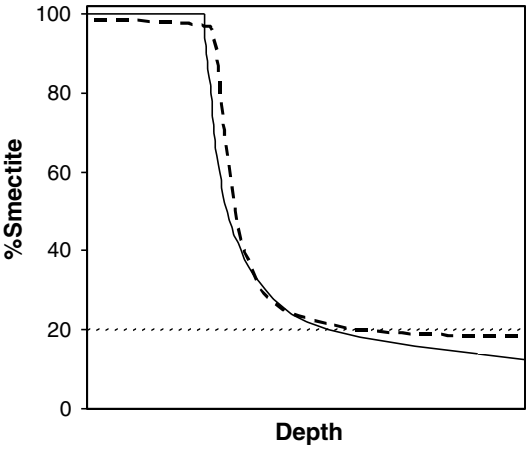

Fig. 1. Percent smectite layers in I–S vs. depth. The dash-line curve is a representation of the typical shape found in sedimentary sequences. The straight dash line marks the limit of illitization also found commonly. The solid line is the result of a model using the equation $-\mathrm{d}S/\mathrm{d}t = kK^{0.25}S^5$, where K and the temperature increase with depth are constant (see text).

According to this, a kinetic equation of the type shown above with $n > 1$ can describe the entire range of values in a typical % smectite vs. depth plot. All the features in the plot are a natural consequence of the equation and there is no need to invoke either several types of processes and mechanisms of smectite illitization or changes in the variables contained in the equation. A similar equation was proposed by Pytte and Reynolds (1989), in which the K concentration is substituted by the pore-fluid activity ratio K/Na. They derived their parameters by fitting the equation to data from a shale bed penetrated by a basalt dike. They found that several parameters could produce good fitting results but only high-order equations could reproduce conditions of low temperature, long duration alteration. Their best match produced the values $n = 5$ (in S^n) and $m = 1$ (in $[\mathrm{K/Na}]^m$). Elliott et al. (1999) also found that the equation of Pytte and Reynolds (1989) with a high order was the best in modeling illitization of bentonite affected by burial, although they expressed their doubts that such equation is the best model for all types of illitization sequences. Altaner (1989) coupled diffusional rates of K in a bentonite bed with illitization rates, in order to model the illite-layer proportion distribution in I–S within the bentonite bed. He used kinetic parameters derived from 1-, 4-, 5- and 6-order kinetic equations, and found that only the parameters from 5- and 6-order equations reproduced the illitization patterns. Thus, when considering kinetic equations of the type described here, high-order equations have proved frequently the most successful to describe illitization in natural systems. These equations also have the advantage that they can represent the entire range of illitization invoking a single mechanism or process.

Several models of smectite illitization have been developed from experimental studies using first-order (Eberl and Hower, 1976; Roberson and Lahann, 1981; Roaldset et al., 1998) and second-order kinetic equations (Huang et al., 1993). These studies used the K-exchanged products extracted from the reactors to measure expandability using X-ray diffraction (XRD) after ethylene-glycol (EG) treatment. However, it has been shown that exchange of such products with Ca, Na or Mg produce re-expansion of a large proportion of layers (Whitney and Northrop, 1988; Cuadros and Linares, 1996). Chemical and spectroscopic data support the fact that these re-expanding layers have a smectitic nature (Cuadros and Linares, 1996; Mosser-Ruck et al., 1999). Thus, data from K-exchanged I–S products are not reliable for kinetic studies. Even so, Whitney and Northrop (1988) tested 1- and 2-order kinetic equations on their XRD results from K- and Na-exchanged products and both failed to match the data, indicating a

higher order. The study by Howard and Roy (1985) differs from the previous ones in that they carried out their experiments in Na/Ca-rich solutions. They analyzed their products by XRD as they were extracted from the reactors (Na/Ca-exchanged) and after K-saturation. They observed that the Na/Ca-products did not show apparent development of layer collapse but the K-exchanged products did. They used their results from the K-exchanged products to study the illitization kinetics and applied a first-order kinetic equation. Evidently, their samples underwent an increase of the layer charge, but the collapsed layers in the K-products cannot be called illite as they were cation-exchangeable. It is perhaps for this reason that they do not refer to illitization but to smectite alteration. Bell (1986) showed that the difference in expandability of natural I–S in its original form and after K-exchange can be as high as 30%. Obviously, smectite and illite have a heterogeneous layer charge. Both types of layers can have a range of this layer charge. It is necessary to establish a boundary differentiating between the two, and this must be the ability to exchange the interlayer cations and expand in response to EG treatment when exchanged with cations such as Ca, Mg, Na or Li. The problem has been further discussed (Meunier et al., 2004; Mosser-Ruck et al., 2005) pointing out the development of high-charge smectite (or vermiculite) layers that can be identified using interlayer cations of different hydration ability and both air-dry and EG-solvation treatments, and that the type of EG-treatment (vapor or liquid) may affect the swelling behavior. However, the previous discussion suffices for the purpose of my argument.

Other authors have also used first-order kinetic equations from natural I–S sequences. Inoue et al. (1992) simply assumed such type of equation without deriving it from their data. Hillier et al. (1995) did derive their equation from their data, but it fails to reproduce the change in slope of % smectite vs. depth at low smectite content. As indicated above, high-order equations can reproduce the change in slope at low smectite content that is typical in I–S conversion series.

The plot in Fig. 1 corresponds to a simple situation in which K concentration, the thermal gradient and the sedimentation rate are constant (i.e., the increase of temperature with depth is constant). Obviously, these may change over time and this complicates the pattern of % smectite vs. depth. Even so, some times it is possible to recognize several stages, within the complete series, which mark changes in the physico-chemical conditions of the sediments (see below). The pattern of these stages can be reproduced using a high-order kinetic equation as described here. At the same time, there can be other complications caused by late local retrograde alteration, which would introduce a group of I–S samples with an anomalously high smectite layer proportion. This fact can be more or less evident depending on several factors. In some cases it can blur the actual illitization pattern. Another complication may be caused by changes in the illite/smectite layer proportions of the detrital smectite or I–S. However, one of the features of an illitization reaction obeying a high-order kinetic equation is that, unless the layer proportion changes are large, they will affect the illitization patterns only if the corresponding sediments were deposited recently (i.e., they are at the top of the sequence). This is because the reaction rate depends on the proportion of smectite layers in I–S and thus is faster for the more smectite-rich I–S. After some time, then, the original differences are wiped out. Finally, other complications of the illitization sequence may be produced by folding and faulting of the sediments that does not affect a vertical sequence uniformly.

3. Potassium concentration

Potassium concentration is the most problematic variable in the modeling of the smectite illitization kinetics. This value is seldom available and present measured values may not correspond to the actual values during the illitization period. Besides, K concentration is not the actual variable modifying the reaction kinetics, as other dissolved cations compete with it for the interlayer sites. Cations such as Ca, Mg or Na preclude or slow down the illitization reaction. There is abundant experimental evidence of this fact (e.g., Eberl et al., 1978) and in certain favorable cases there is also positive evidence from field samples that lack of K availability or a large concentration of other cations stopped illitization (Masuda et al., 1996). Thus, a more accurate way of representing this variable is some sort of ratio between the concentrations of K and other cations. However, this ratio would need to include a function of the selectivity of smectite layers for the several cations. A further complication is that this selectivity depends on the hydration state of the smectite layers, and that the interlayer cation affects such hydration state. Hence, we may expect that this selectivity is not the same at different burial depths. According to this discussion, K concentration needs to be understood as an "effective concentration" which depends on the factors enumerated above. The effective K concentration will only be equivalent to the K concentration in systems where K is in much higher concentration than other dissolved cation, as is the case of many experimental studies. When the equations obtained from such studies are applied to geologic systems we can expect that the values introduced as effective K concentration are lower, perhaps much lower, than the actual K concentrations measured or that could be expected.

Sodium is readily displaced from the smectite interlayer by K, but Mg and Ca have a greater affinity than K for interlayer sites in the range of cation concentrations found in interstitial fluids (Fletcher and Sposito, 1989; Verburg and Baveye, 1996). As interstitial water in most sediments contains less Mg than Ca or Na (Brownlow, 1996; Langmuir, 1997), and as Na is a weak competitor with K for the smectite interlayers, it is Ca the main cation that will have a slowing effect on the illitization reaction. When assessing the value of the effective K concentration, atten-

tion should be given to the presence of calcite, as the most common Ca-bearing mineral. Potassium feldspar is the corresponding K-bearing mineral to consider. However, their corresponding concentrations in the sediments are not a direct indication of what the relative concentrations of K and Ca are, as these depend on the solubility of the corresponding minerals, which depend also on grain size. Besides, it is difficult to interpret whether the relative decrease of calcite down in a sedimentary sequence should be translated into a decrease of dissolved Ca. If the calcite relative decrease is due to lower calcite input into the sediment, one would infer a concomitant lower dissolved Ca. But the calcite decrease could be due to calcite dissolution, in which case it would produce higher dissolved Ca within the range allowed by calcite saturation. Occasionally, Ca-bearing phases other than calcite will be present too. Na-bearing minerals would need to be considered only if they are sufficiently abundant and likely to cause Na to be the dominant dissolved cation.

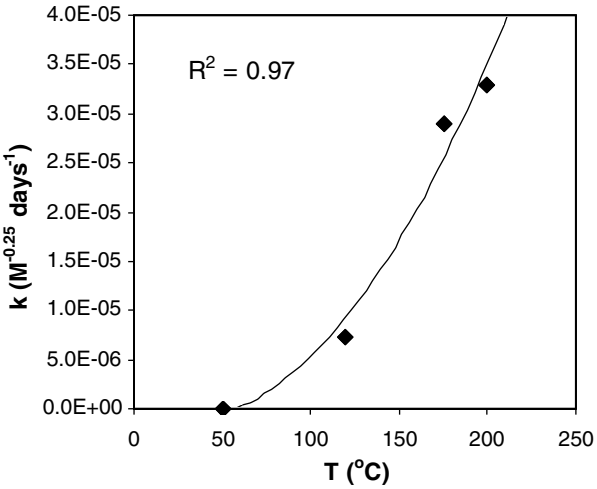

Fig. 2. Value of the rate constant (k) calculated at different temperatures by Cuadros and Linares (1996). The value at 50 °C is assumed. The curve is a polynomial regression of the four data points. It provides a value of k for any temperature used in the model.

4. Kinetic equation used for the modeling

I used the kinetic equation from Cuadros and Linares (1996) derived from experimental alteration of smectite samples in K solutions at temperatures 60–200 °C: $-\mathrm{d}S/\mathrm{d}t = kK^{0.25}S^n$. The proportion of smectite, S, is a fraction and has no units, t is expressed in days, and K in M. The value of the exponent of S could not be determined, as the reaction progressed very little (maximum transformation of ~0.3%; the progress of the reaction was determined from chemical rather than XRD data). Considering that Pytte and Reynolds (1989) and Altaner (1989) were successful in their models using $n = 5$ (see discussion in Section 2), I chose this value. Thus, the formula used was the integrated version of the above equation: $(1/S_f^4) - (1/S_i^4) = 4kK^{0.25}t$, where the subscripts f and i indicate final and initial fraction of smectite layers in I–S at any step of the reaction.

The value of the rate constant, k, is a variable depending on the temperature. Cuadros and Linares (1996) performed their experiments at 60, 120, 175 and 200 °C. They did not detect illitization at 60 °C. The onset of smectite illitization found in the literature spans from ~70 °C (Jennings and Thompson, 1986) to ~100 °C (Inoue et al., 1992). The actual value may be <70 °C, as the presence of very few illite layers in I–S are difficult to detect and so they may not have been observed. I used the three values of k from Cuadros and Linares (1996), obtained for $n > 1$, corresponding to the temperatures 120–200 °C. To these I added the assumed value $k = 0$ for 50 °C, and calculated the correlation between temperature and k values (Fig. 2). I then used the regression equation to calculate the k values that are used in the model. The equation obtained is $k = 1.213 \times 10^{-9}T^2 - 6.608 \times 10^{-8}T - 2.033 \times 10^{-7}$ with the units $\mathrm{M}^{-0.25}$ days^{-1}, where T is the temperature in °C. With this equation, $k > 0$ for $T > 57.4$ °C. If the data point at 50 °C were not added, the regression of the three k values from Cuadros and Linares (1996) would yield an illitization onset at 93 °C, which is with all probability too high given that the reaction has been observed to start at lower temperatures. The assumed value of $k = 0$ is not valid according to kinetic theory, as reaction rates do not become zero but rather the reaction rates of the opposite reactions become of equal value. However, the kinetic equation used here is only empirical and does not describe the actual mechanism of the process. Thus, k is an overall value that integrates rate constants of several individual processes or steps.

The actual calculations of % smectite vs. depth were performed in the following way. The depth range was divided in steps of 20 m. I assigned an effective K concentration (K) and temperature to each step. The temperature was taken from the measured geothermal gradient in each well studied and I assumed an initial (surface) temperature of 20 °C in all cases, as all wells are onshore. For each depth step there is a corresponding time lapse, obtained from the measured sedimentation rate and time elapsed after sedimentation stopped. I assumed a constant I–S composition of the original sediment throughout the vertical sequence. This value varies between 100% and 75% smectite layers, and was taken from the experimental data in the shallow sediments. Given that all the original sediments are smectite-rich and the characteristics of the kinetic equation, possible differences in the I–S composition affect the model only at shallow depths. The K value is the only variable for which there is no information. It was assigned to fit the experimental data, although changes of K were allowed preferably when there were indications of other changes in the sedimentation conditions, e.g., changes in the sedimentation rate, geothermal gradient or bulk mineralogy, with special attention to calcite concentration. The K values are in M, as in the equation by Cuadros and Linares (1996), although, as discussed above, it does not represent a simple K concentration. Finally, the decrease of smectite

proportion was calculated for each depth step. For the cases where the sedimentation rate changes with time, the calculations were divided in several sequences to allow the coupling of the right sedimentation rate and temperature (or depth) in each part of the well section. Compaction of the sediments was not considered.

Although one of the variables is adjusted to fit the data, there are several tests to the validity of the model. (1) The position of the onset of illitization, as it is independent of K, the adjusted variable (provided that $K > 0$). (2) The shape of the illitization curve, because it is controlled by the whole of the equation, where K is only one of the variables. If the calculated values can be adjusted properly to the slope changes in the experimental pattern, the test provides a positive result. (3) The likelihood of the assigned K values. This is a test difficult to assess because the exact form of the effective K concentration variable is not known. However, I discuss it here using mineralogical and chemical data where they are available. I comment on the errors implicated in the calculations after the results section.

5. Results

5.1. SW Texas

The first model presented is the one that required the simplest input parameters. It does not correspond to a single well but it was included because it is very illustrative owing to the simplicity of the input parameters. Boles and Franks (1979) studied illitization in the sandstones and shales of the Wilcox group in SW Texas. I only used the shale data, as the sandstone data cover a very narrow range of illitization. The data correspond to the <1 μm rock fraction. The samples were collected from a number of wells most of them located within a radius of 8 km. Table 1 indicates the input variables. Where not mentioned otherwise, for this and the other modeled sequences, the thermal gradient and sedimentation rate were taken from the publications in Table 1. In this first case, two of the wells have a thermal gradient of 31 °C/km (Boles and Franks, 1979) but these correspond to the shallowest samples, with lower temperatures, and their effect on the calculations is small. Boles and Franks (1979) provided their data as % smectite vs. temperature. I transformed the data into % smectite vs. depth, using the thermal gradient of 40 °C/km (Table 1), which is the gradient measured in all except the two mentioned wells (Boles and Franks, 1979). This causes a slight change in the depth of the shallower samples. The change is small precisely because they are located in the shallowest sediments. The general pattern of illitization in Fig. 4 of Boles and Franks (1979) is identical to that in Fig. 3a of this paper. The sedimentation rate was obtained from Galloway (1990) and Murray (1960). They provide depth–age data for a section across the Rio Grande embayment (Galloway, 1990) and a line in the direction NW–SE near the relevant wells (Murray, 1960). Their depth–age data can be approximated with a single linear equation ($R^2 = 0.97$) and thus the depositional rate was considered constant. One single value of the effective K concentration is sufficient to fit the entire range of data. The only indication about presence of Ca-bearing minerals in Boles and Franks (1979) is that calcite and ankerite are rare in the shales. The effective K concentration values for all the basins will be discussed together at the end.

The illitization curve (Fig. 3a) shows a very steep progression at the beginning, due to the high geothermal gradient. It is not possible to know whether the original sediments contained smectite or smectite-rich I–S, but this does not affect the model because of the high initial illitization rate. Models starting at 100% and ~70% smectite layers fit the data equally well. After the first stage, the reaction rate decreases drastically, due to its high dependence on the proportion of smectite layers, as discussed above. The calculated rates match the experimental data very well, including both the onset of illitization and the progression curve. A group of samples at ~4000 m plot above the illitization trend. This is most probably due to faulting and the consequent downwards displacement affecting some of the deep sections of the Wilcox group (Galloway, 1990), causing these sections to have been at the corresponding depth for a shorter time. This sequence model is a key test for the validity of the equation as it uses one single value of each variable for the entire sequence, which means that the total number of input values is the minimum possible. Also, the homogeneous conditions along the sequence, except the faulting, minimize the alterations induced to the illitization pattern.

5.2. Los Angeles

Data for I–S progression in a location near Whittier (Orange County, California) are provided by Velde and Vasseur (1992). The rocks are mudstones. The sedimentation rate provided by the authors was compared with that for the same well in Velde and Ijima (1988). I found that there is a good match between the two above 4000 m and that the deepest age–depth data point indicates a lower deposition rate. However, this latter sedimentation regime could not affect illitization measurably, as it operated on the studied samples only for a short period when the corresponding sediments were very shallow (~500 m). The geothermal gradient provided by Velde and Vasseur (1992) of 27.5 °C produces a calculated illitization onset which is at a much shallower depth than that of the experimental data, and thus was considered too high. In fact, the gradient actually measured had been modified by Velde and Ijima (1988) because they considered that the temperature acquired at the bottom of the well was low due to incomplete equilibration after introducing the probe. I used the thermal gradient obtained from the direct experimental data (Table 1; Velde and Ijima, 1988). Three effective K concentrations were used in the model, although two of them only affect the two deepest samples. The illitization pattern in this basin (Fig. 3b) is quite different from the previous

Table 1
Values of the variables used in the models

Authors	Location	Thermal gradient (°C/km)	Age range (My)[a]	Age of surface sediments (My)[b]	Age of oldest sample (My)[b]	Sedimentation rate (m/y)	Effective K conc. (M)[c]
Boles and Franks (1979)	SW Texas	40	43.6–94.3	36.7	81.8	1.04×10^{-4}	5×10^{-17}
Velde and Vasseur (1992)	Los Angeles	20	1.7–5.0	1.35	4.5	14.75×10^{-4}	10^{-21} (0–4060 m) 10^{-20} (4060–4460 m) 10^{-18} (4460–5500 m)
Freed and Peacor (1992)	S central Texas	35 (0–1420 m) 16 (1420–3280 m) 45 (3280–5500 m)	23.8–65.0	18.0	65.5	0.779×10^{-4}	10^{-21} (0–1420 m) 5×10^{-22} (1420–2240 m) 10^{-13} (2240–5500 m)
Hower et al. (1976)	SE Texas	21 (0–3300 m) 39 (3300–5500 m)	20.4–32.7	18.1	34.1	3.26×10^{-4}	10^{-23} (0–3000 m) 10^{-18} (3000–4000 m) 10^{-21} (4000–5500)
Velde and Vasseur (1992)	S central Texas	42	55.5–160	43.6	137	0.86×10^{-4} (0–1880 m) 0.39×10^{-4} (1880–5500 m)	10^{-25} (0–2200 m) 10^{-23} (2200–2620 m) 10^{-22} (2620–2820 m) 10^{-16} (2820–2940 m) 10^{-13} (2940–3080 m) 10^{-10} (3080–5500 m)
Perry and Hower (1972)	SE Texas	25 (0–2736 m) 39 (2736–5500 m)	16.0–31	15.5	31.3	2.3×10^{-4} (0–2500 m) 13.14×10^{-4} (2500–5500 m)	7×10^{-21} (0–2500 m) 10^{-19} (2500– 3080 m) 10^{-13} (3080–3240 m) 10^{-24} (3240–5500 m)
Awwiller (1993)	S central Texas	40	40.2–57.8	35.7	57.6	2.7×10^{-4} (0–1800 m) 0.84×10^{-4} (1800–2800 m) 5.14×10^{-4} (2800–5500 m)	2×10^{-24} (0–2260 m) 2×10^{-25} (2260–2880 m) 2×10^{-20} (2880–2960 m) 2×10^{-17} (2960–5500 m)
Hillier et al. (1995)	Hungarian Plain	35	0.18–11.0	0.19	10.2	3.26×10^{-4} (0–550 m) 1.06×10^{-4} (550–950 m) 5.63×10^{-4} (950–2400 m) 8.14×10^{-4} (2400–5500 m)	10^{-17} (0–1720 m) 10^{-19} (1720–2360 m) 1.5×10^{-18}–5×10^{-17} (2360–2500 m) 5×10^{-16} (2500–3100 m) 5×10^{-15}–5×10^{-13} (3100–3160 m) 10^{-10} (3160–5500 m)

The values in parenthesis are the depth ranges to which the corresponding variable applies.
[a] Range of the available sediment ages from where the sedimentation rates were calculated.
[b] From the calculations.
[c] The calculations were performed up to 5500 m in all cases.

one. The faster sedimentation rate (i.e., young sediments), lower thermal gradient and lower effective K concentration produce a curve of different shape and a much smaller extent of illitization.

5.3. S central Texas (1)

Freed and Peacor (1992) studied shale samples from a well in the De Witt County, Texas. The geothermal gradient changes twice along the section. Using four age–depth datapoints (boundaries between sediments from different stratigraphic units), the sedimentation rate could be approximated ($R^2 = 0.98$) to a single value. Three values of the effective K concentration were used. The first change coincides with the first variation of the geothermal gradient. No bulk mineralogical analyses of these samples were found. However, I observed that the pattern of effective K concentration needed to model this I–S sequence was sim-

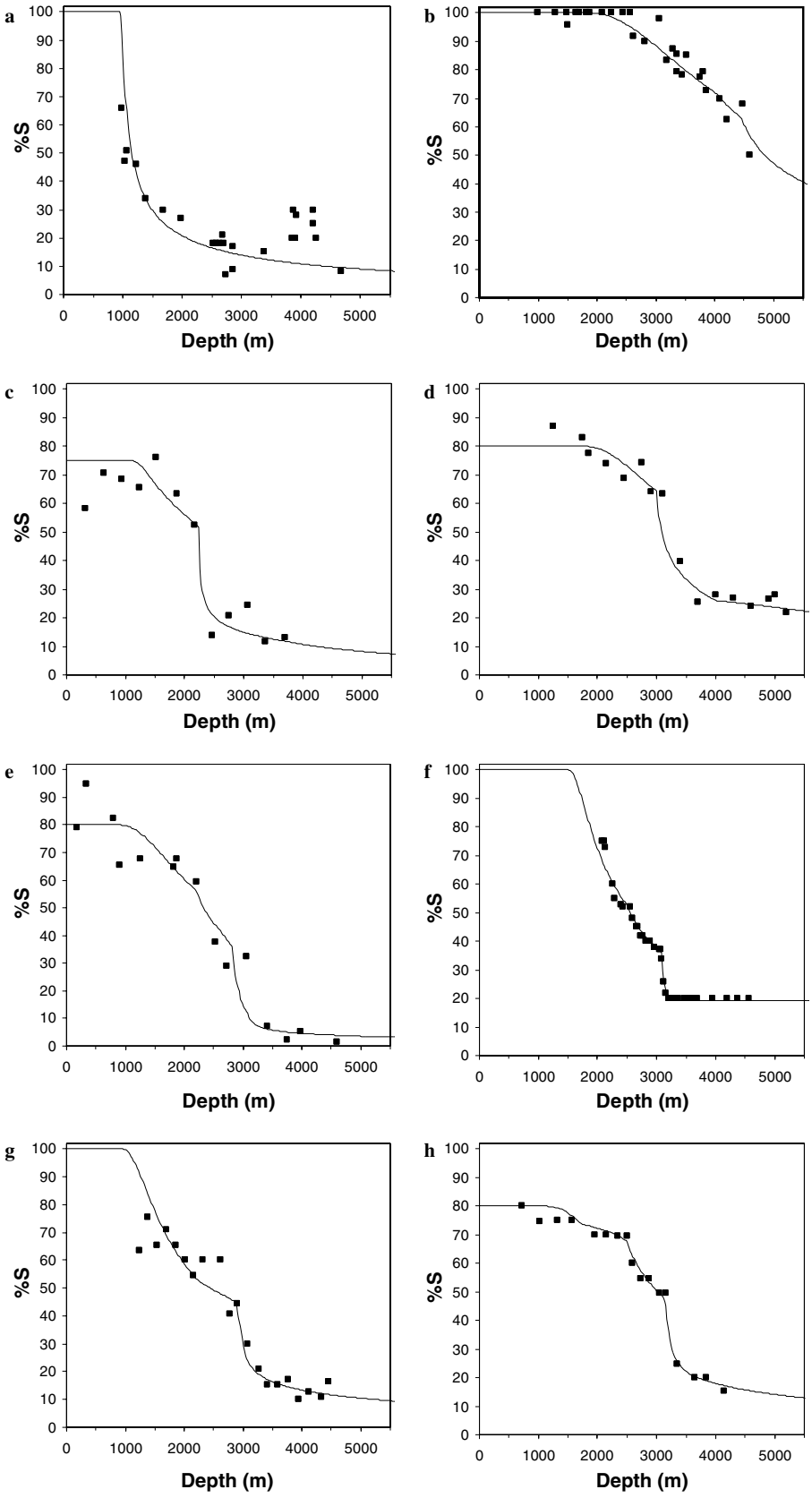

Fig. 3. Percent smectite layers in I–S vs. depth for the modeled sequences. The data points are the experimental data and the lines are the calculated values. (a) Boles and Franks (1979); (b) Velde and Vasseur (1992), Los Angeles; (c) Freed and Peacor (1992); (d) Hower et al. (1976); (e) Velde and Vasseur (1992), Texas; (f) Perry and Hower (1972); (g) Awwiller (1993); (h) Hillier et al. (1995).

ilar to that in Awwiller (1993, see below), a well located ~11 km from this one. Thus, the relative mineralogical changes of the sediments along the two sections is probably similar. The experimental data points show considerable dispersion. The original sediments seem to contain ~25% illite layers. The most clear feature shown by the experimental data is the large decrease of smectite layers at ~2300 m, which is produced in the simulation by the increase of effective K concentration at 2240 m.

5.4. SE Texas (1)

Hower et al. (1976) investigated illitization in shale cuttings from a well in Harris County, Texas. They measured illite layer proportions in I–S from several size fractions, 2–0.5, 0.5–0.1 and <0.1 μm, and they provided the corresponding relative proportions of these fractions in the total <2 μm size fraction, although not for all samples. Using these values, I calculated the total proportions of illite and smectite in the entire <2 μm fraction. For those samples for which the relative proportions of the several particle size fractions were not provided, I observed the trends (increasing or decreasing) for each size fraction with depth and interpolated their values. In spite of the uncertainty involved, I believe it is reasonable to use this procedure to simplify the data and make them directly comparable to data from other locations. The differences in % illite measured by Hower et al. (1976) between the extreme fraction values, 2–0.5 and <0.1 μm, are 5–20%, with lower % illite results for the 2–0.5 μm size fraction. The 0.5–0.1 μm size fraction produced intermediate values in most cases. All the fractions follow a similar illitization pattern.

The depth–temperature data in Hower et al. (1976) show a linear progression from 3500 m downwards but a data point at 1112 m shows a clear departure from linearity. If the data are divided in two groups, 0–3500 m and 3500–5776 m, the linear equation corresponding to the first group intersects the temperature axis at 16 °C, which is very close to the present mean surface temperature of 23 °C (Burst, 1969). Thus, it is very likely that there are two geothermal gradients. I used the regressions from the temperature–depth data to calculate their values and the inflection point (intersection of the two lines). The sedimentation rate was taken from the age–depth values given by Aronson and Hower (1976) for the same well. The whole range of the relevant sediments can be reasonably adjusted to a single sedimentation rate ($R^2 = 0.97$) and thus I used only one value. The three regions of effective K concentration follow the pattern of calcite abundance. In the first one (0–3000 m) there is a high calcite content (10–30 wt%). In the second region (3000–4000 m), calcite content decreases progressively and it is very low in the third stage (4000–5500 m). Hower et al. (1976) attribute this decrease to calcite dissolution and, accordingly, dissolved Ca could have been higher here. However, K-feldspar content in the sediment follows a very similar pattern. If this mineral dissolved together with calcite, the dissolution of these minerals would have had the opposite effect on the effective K concentration. Aronson and Hower (1976) provide the wt% K_2O content in the whole rock samples. This content is constant up to 3000 m, then increases progressively up to 4000 m and then remains constant or decreases slightly. These data can be used in conjunction with the previous ones in order to assess the trends of the effective K concentration. They indicate that there was a net gain of K in the second stage here considered (3000–4000 m), and thus it is reasonable to assume a larger effective K concentration. In the last stage, there is no further gain of K in the sediment, which probably means that the amount of K available for the illitization reaction decreased again, as part of the K in the sediment is in the illite layers of I–S.

It seems that the original sediment contained I–S with ~20% illite layers, rather than smectite, as the relatively high sedimentation rate and relatively low geothermal gradient set the illitization onset at ~1900 m (Fig. 3d). This was followed by a slow reaction progress, accelerated at 3000 m by the combination of the higher geothermal gradient and effective K concentration, and decelerated again at 4000 m due to the lower K availability.

5.5. S central Texas (2)

The data for this series were taken from Velde and Vasseur (1992). They indicated that the series is from Peeler, Atascosa County, in south Texas. However, I could not find a locality of that name (Peeler) in this county. The samples are shales. There is scattering at the top of the series (Fig. 3e) and it is difficult to know the original illite content in I–S. As in the previous well, the thermal gradient and sedimentation rate suggest ~80% illite. Velde and Vasseur (1992) indicate a geothermal gradient of 36 °C/km, which is too low to allow a good fit with the experimental data. In other words, the sedimentation rate and this thermal gradient cannot produce the steady progress of illitization observed at the top of the sequence. Burst (1969) provides a contour map or geothermal gradients of the US Gulf Coast. The available data cover the area south and east next to Atascosa but not the county itself. I assumed the geothermal gradient found in the closest proximity. In this location, the sedimentation rate for the greatest part of the sequence (1880–5500 m) is constant (the depth–age data produce a linear correlation with $R^2 = 0.99$) but it was significantly slower in the surface sediments (0–1880 m). It was necessary to use two sedimentation rates because the latest one has a great effect on the medium-depth and bottom sediments, as it dictates the velocity at which they subside in the regions of higher temperature, which are more sensitive to variations of the other physico-chemical conditions.

The effective K concentrations needed to match the experimental points have the highest variation found in this study, increasing from top to bottom. If the thermal gradient was higher, at least at the bottom, than the one used here of 42 °C/km, some of the values of the effective K con-

centration could be reduced. Unfortunately, there are no mineralogical data to contrast these results. This sequence contains the oldest sediments modeled here. Interestingly, in spite of the old sediment age and the seemingly high thermal gradient and interstitial K concentration the illitization reaction does not proceed to completion.

5.6. SE Texas (2)

Perry and Hower (1972) studied shales from two wells, in Texas and Louisiana. As I could not collect information about sedimentation rates in the latter, only the former was modeled. The well is located near Galveston. The authors indicate a geothermal gradient of 31 °C/km. However, Perry and Hower (1970) provide a depth–temperature plot for the same well and I used these data. The lower part of the section (2900–5500 m) can be approximated accurately with a single gradient ($R^2 = 0.97$) but the top section indicates a lower value, as the extrapolation of the mentioned gradient to the surface produces an unrealistic temperature of −18 °C. I assumed a surface temperature of 20 °C and calculated two geothermal gradients (Table 1). Indeed, the single value provided by Perry and Hower (1972) is intermediate between the two used in my model. The sedimentation rates were obtained from Ye et al. (1993), who provide depth–age data for Lower Miocene sediments for a NW–SE line near Galveston, and Galloway and Williams (1991), who provide sedimentation rates for the Upper Oligocene (Frio formation) sediments in the Galveston area. The data by Ye et al. (1993) produce a good linear regression ($R^2 = 0.90$) and were approximated to a single sedimentation rate value. The obtained rates were compared with those of Brown et al. (2004, 2005) from complete sections from the Corpus Chirsti area and were in excellent agreement. Also, these rates generate an age of 31 My for the deepest sample, in good agreement with the fact that all samples are from the Frio formation (bottom 30–33 My old). The effective K concentration increases from top to bottom, with a sudden peak at 3080–3240 m. This peak is necessary to explain the sharp decrease of smectite layers observed at this depth (Fig. 3f). At the bottom, the effective K concentration decreases sharply and the reaction stops. However, the model indicates that it is not necessary that the sediments are completely K-depleted to explain the stop of the reaction.

The illitization sequence from this well is very informative because the data points follow each other closely and the scattering is minimum. The experimental data show three steps, each shaped as a back-to-front "j," 2112–2540, 2540–3080 and 3080–4600 m. Each step corresponds to the development of the pattern of illitization where there is no substantial change of the physico-chemical conditions, that is, rapid decrease of smectite layers first and subsequent slow down of the process. A new step indicates that one or some of these conditions changed causing an acceleration of the reaction (Table 1). In the last step there is not only the natural decrease of the slope but also the effect of the decreased K availability (at 3220 m). In the second and third steps, the model could be closely fit to the data points, but not as much in the first one.

5.7. S central Texas (3)

The data are from shale samples in a well in the De Witt County, Texas, provided by Awwiller (1993). The geothermal gradient was obtained from the depth–temperature values at 2100 and 4500 m, plus an assumed temperature of 20 °C at the surface. There are three sedimentation rates, each obtained from well-correlated depth–age values ($R^2 = 0.997$, 0.997 and 0.96). The effective K concentration follows roughly after the values of calcite abundance in the bulk sediment. These are typically ~1 wt% (1200–1800 m), 5–2% (1800–2800 m) and 1–2% (2800–4400 m). Note that the points of calcite abundance variation coincide with those of sedimentation rate change. The effective K concentration decreases where calcite is more abundant. Awwiller (1993) indicates that the present K concentration at the bottom is high (~0.01 M). Thus the final increase of the effective K concentration may not only be due to lower calcite contents but to higher dissolved K.

The upper part of the sequence (Fig. 3g; 1200–2600 m) shows some scattering of the experimental data and it is difficult to assess both the original composition of I–S in the sediments and the actual slope of the illitization pattern. The lower part, however, is well constrained. This lower part is a good example of the steps described in the previous well. As the lower sediments were buried from 2600 to 4400 m the sedimentation rate was constant (2.7×10^{-4} m/y). The calculated effective K concentration increases in a small range of depth at the beginning of this lower part and then becomes constant. Thus, it can also be considered that the chemical conditions were the same in this range of depth.

5.8. Great Hungarian plain

Hillier et al. (1995) modeled the illitization patterns of mudrock sediments from three locations of the Pannonian basin. I modeled only the one with low scattering and covering a wide range of I–S composition. This is the most complicated of the wells modeled here, with four different sedimentation rates. The effective K concentrations are set to fit the data. The only change of this variable with a correspondent alteration of the sedimentation rate is at ~2400 m. Unfortunately, I could not find mineralogical or chemical data for the bulk sediments to contrast the model results. In this sequence, due to the low data point scatter, it is also possible to observe several steps (3 or perhaps 4) in the illitization pattern. As in the previous cases, the deeper steps are more evident.

6. Error analysis

The model contains many variables of whose uncertainty there is no information. Also, it is difficult to assess

uncertainties in assumptions such as considering equal present and past geothermal gradients. However, it is safe to assume that there is an overriding source of error, the determination of %S in I–S. The uncertainty of this variable is probably the largest of those that can be assessed. Accordingly, I provide here an analysis of errors based on it. The values of the rate constant used in the model were calculated from chemical data, assuming a certain stoichiometry for the illitization reaction (Boles and Franks, 1979; Cuadros and Linares, 1996) and using the measured %S in the specimen treated hydrothermally (85%). According to repeated determinations of this value, the uncertainty of %S was ±2%. This uncertainty produces an error of ±10% in the k value.

The determination of %S in I–S in the modeled sequences was carried out using several methods. In most cases, the authors provided an assessment of the uncertainty of this value, in three cases there was no error provided (Boles and Franks, 1979; Freed and Peacor, 1992; Hillier et al., 1995). For these three sequences, I used the most common uncertainty reported of ±5%. The values are listed in Table 2. In the case of the sequence of Hower et al. (1976), the authors measured %S values from three particle size ranges and assessed a variable uncertainty (±2 to ±7%). I did not used in the model the %S values measured by the authors, but a weighted value calculated from the several proportions of the three particle size ranges. Thus, I used their maximum uncertainty, to provide for error accumulation in the weighted %S values.

The %S errors in Table 2 were used to calculate maximum uncertainties in the effective K concentration. That is, the models were fitted assuming a consistent displacement of all the %S values along the sequence, corresponding to the errors. This provides a maximum and minimum K value. This calculation was performed for the sequence of decreasing %S at 10% steps. The approximate ranges of depth to which they correspond are also indicated in Table 2 in order to allow comparison with the calculated K values in Table 1. For every step, the depth range is that between the figure in the previous step and that in the corresponding step. However, the depth sequence is less detailed in the error assessment in Table 2 (fewer steps are shown) than in the effective K concentration in Table 1. From this assessment, it can be observed that the effective K concentration is quite sensitive to the actual %S values, which is not surprising as the K parameter has a tremendous range of variation. Typical differences between minimum and maximum values are of four orders of magnitude. The series from Velde and Vasseur (1992) in Los Angeles presents the lowest margins of K variation. This is due to the fact that the extent of illitization is the lowest and the progression with depth has the smoothest variation. In general, the margin of uncertainty is greater at greater depths, because the reaction rate has a great dependence on %S, slowing down towards lower %S values, so that a similar variation in %S needs larger K variations in the bottom of the sequence than at the top. The extreme example of this effect is the bottom of the series from Velde and Vasseur (1992) from Texas, which reaches the lowest %S values and thus produces a maximum K difference of 10 orders or magnitude.

As indicated, this error assessment provides a maximum range of uncertainty and assumes a consistent bias in the errors on both sides of the calculated effective K concentration. Probably, this would not be the case in the real measurements and this means that the real analytical errors would not produce a uniform displacement of the datapoints up or down in the %S vs. depth plots, but a random vertical displacement of variable extent within the calculated range. The best way of assessing the reliability of the %S measurements is the degree of the data dispersion. Thus, the data from Perry and Hower (1972, Fig. 3f) are probably the most accurate, and those from Freed and Peacor (1992, Fig. 3c) the least. However, in all the sequences it is possible to observe the same features in the illitization progression, with straight and curved stretches. Thus, it is reasonable to conclude that the actual uncertainties do not blur the shape of the illitization curve and that the observed features do correspond to real physico-chemical characteristics of the modeled sequences.

7. Discussion

The effective K concentration is the only variable used in these calculations not directly available. In order to assess the accuracy of the kinetic equation used here, it is first necessary to discuss the values that were used in the model. The two initial impressions are that the values are generally very low and that they change dramatically (up to 15 orders of magnitude). These two features seem unrealistic at first sight. For example, Langmuir (1997) compiles threshold values of ion concentrations in shales, and the value for K is $\sim 7 \times 10^{-4}$ molal, much higher than many of those used here. However, as previously discussed, the effective K concentration depends also on the competing effect of other cations, especially Ca. Threshold concentrations in shales for Ca, Mg and Na are 0.015, 0.01 and 0.063 molal, respectively (Langmuir, 1997), all of them well above the value for K. The actual concentrations may be higher, but this comparison indicates that the effective K concentration may be well below the actual concentration in the interstitial fluids.

Fig. 4a shows the effective K concentrations used in my models at the different depths. There is information about the bulk chemical composition for three of the locations studied (Perry and Hower, 1972; Hower et al., 1976; Awwiller, 1993). Potassium and Ca are the main competitors for the interlayer positions, because Na is more easily displaced and Mg enters the octahedral sheet of phyllosilicates. Verburg and Baveye (1996) show that, in the K/Ca exchange in montmorillonite, Ca is twice as effective as K in occupying the adsorption sites, for most of the range of K/Ca ratio in solution. More specifically, the equivalent ratio K_{eq}/Ca_{eq} in montmorillonite is approximately half of

Table 2
Errors in the determination of %S in I–S and the corresponding maximum variation of the effective K concentration at decreasing %S

%S error:	Boles and Franks, 1979 ±5%[a]	Velde and Vasseur, 1992, LA ±5%	Freed and Peacor, 1992 ±5%[a]	Hower et al., 1976 ±7%	Velde and Vasseur, 1992, Tx ±5%	Perry and Hower, 1972 ±5%	Awwiller, 1993 ±5 to ±8%[b]	Hillier et al., 1995 ±5%[a]
%S	K (M)	K (M)	K (M)	K (M)	K (M)	K (M)	K (M)	K (M)
100	5×10^{-15} 5×10^{-19}	2×10^{-21} 10^{-22} (0–2560 m)				4×10^{-20} 2×10^{-21} (0–1660 m)	8×10^{-24} 5×10^{-25} (0–1160 m)	
90	5×10^{-15} 5×10^{-19}	2×10^{-21} 10^{-22} (3200 m)				4×10^{-20} 2×10^{-21} (1800 m)	8×10^{-24} 5×10^{-25} (1360 m)	
80	5×10^{-15} 5×10^{-19}	2×10^{-21} 10^{-22} (3800 m)	5×10^{-21} 5×10^{-23} (0–1100 m)	10^{-22} 10^{-24} (0–2380 m)	6×10^{-25} 4×10^{-27} (0–1360 m)	4×10^{-20} 2×10^{-21} (1960 m)	8×10^{-24} 5×10^{-25} (1560 m)	4×10^{-17} 10^{-18} (0–1660 m)
70	5×10^{-15} 5×10^{-19}	10^{-21} 10^{-21} (4340 m)	5×10^{-21} 5×10^{-23} (1580 m)	10^{-22} 10^{-24} (2960 m)	6×10^{-25} 4×10^{-27} (1800 m)	4×10^{-20} 2×10^{-21} (2140 m)	8×10^{-24} 5×10^{-25} (1800 m)	6×10^{-19} 10^{-18} (2540 m)
60	5×10^{-15} 5×10^{-19}	10^{-20} 10^{-20} (4660 m)	5×10^{-21} 5×10^{-23} (2060 m)	10^{-16} 3×10^{-20} (3040 m)	6×10^{-25} 10^{-26} (2220 m)	4×10^{-20} 2×10^{-21} (2420 m)	5×10^{-23} 2×10^{-26} (2110 m)	5×10^{-15} 5×10^{-17} (2820 m)
50	5×10^{-15} 5×10^{-19}	10^{-17} 10^{-18} (5140 m)	5×10^{-21} 5×10^{-23} (2240 m)	10^{-16} 3×10^{-20} (3160 m)	5×10^{-23} 10^{-24} (2480 m)	5×10^{-18} 2×10^{-21} (2700 m)	5×10^{-24} 5×10^{-26} (2880 m)	5×10^{-15} 5×10^{-17} (3160 m)
40	5×10^{-15} 5×10^{-19}	10^{-17} 10^{-18} (5500 m)	5×10^{-21} 5×10^{-23} (2260 m)	10^{-16} 3×10^{-20} (3440 m)	10^{-21} 10^{-23} (2820 m)	10^{-18} 2×10^{-21} (3080 m)	10^{-12} 10^{-20} (2950 m)	5×10^{-10} 5×10^{-12} (3210 m)
30	5×10^{-15} 5×10^{-19}		5×10^{-11} 5×10^{-15} (2360 m)	10^{-16} 3×10^{-20} (4480 m)	10^{-15} 10^{-18} (2860 m)	10^{-11} 2×10^{-15} (3130 m)	10^{-12} 10^{-20} (3060 m)	5×10^{-10} 10^{-12} (3380 m)
20	5×10^{-15} 5×10^{-19}		5×10^{-11} 5×10^{-15} (2980 m)	10^{-19} 10^{-23} (5600 m)	10^{-15} 10^{-18} (2990 m)	10^{-24} 10^{-24} (5500 m)	10^{-12} 10^{-20} (3680 m)	3×10^{-8} 10^{-12} (4700 m)
10	5×10^{-15} 5×10^{-19}		5×10^{-11} 5×10^{-15} (5500 m)		10^{-5} 10^{-15} (3780 m)			
0					10^{-5} 10^{-15} (5500 m)			

The approximate depth ranges at which they occur are indicated in parenthesis.
[a] Assumed, not provided by the authors.
[b] Awwiller (1993) estimated that the error increased with decreasing %S.

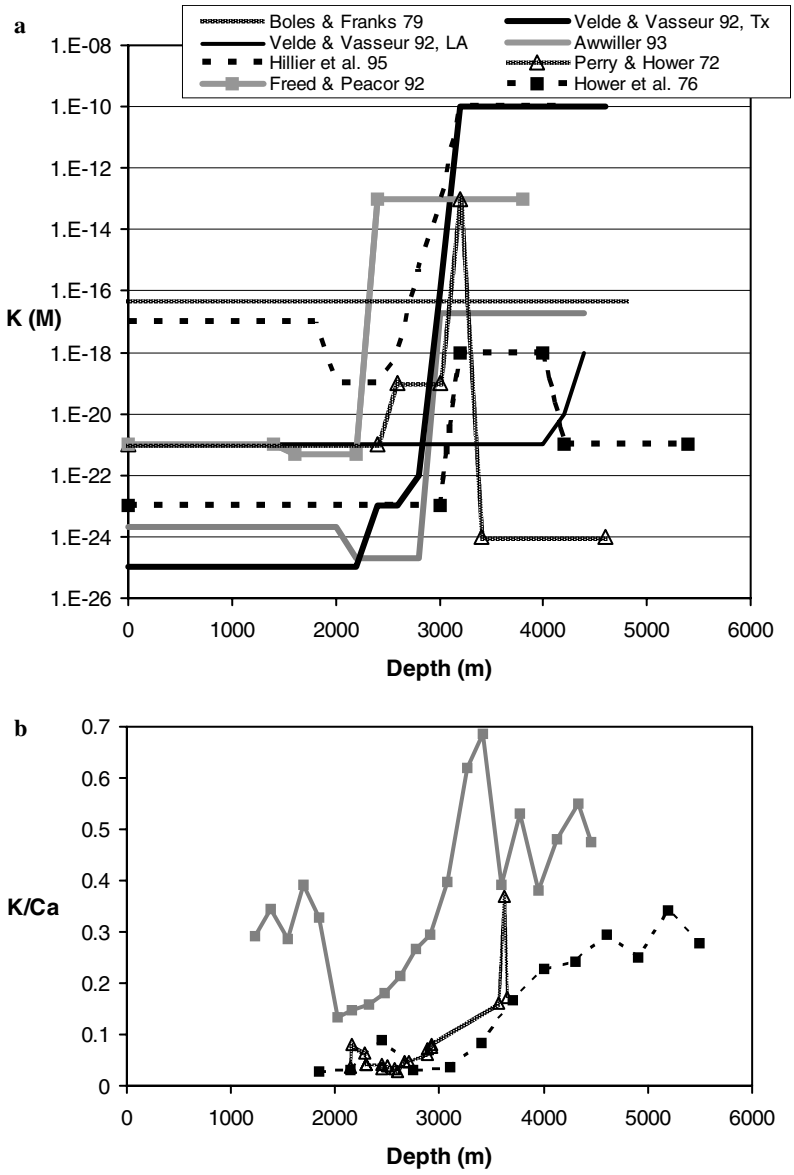

Fig. 4. Variation of the effective K concentration used in the models (a) and of the ratio $K_{eq}/2Ca_{eq}$ obtained from the chemical composition of the sediments (b, see text) with depth. The K/Ca ratio represents an approximation to the relative change of the effective K concentration within the sequence. The line types in the box apply to both plots.

the same ratio in solution, for the range $0 \leqslant [K_{eq}/Ca_{eq}]_{sol} \leqslant 0.8$. I converted the wt% values of K_2O and CaO of the whole rock from the three mentioned locations in this study into the corresponding equivalent values and then calculated the ratio $K_{eq}/(2Ca_{eq})$. The number of Ca equivalents is multiplied times two because Ca is twice as effective in the competition for the interlayer sites of smectite. Fig. 4b shows a plot of this ratio vs. depth. The comparison of Figs. 4b and a, for the corresponding wells, shows that the main features in Fig. 4b can be observed in Fig. 4a. The relative values change approximately at the same depth. Especially striking is the peak in the data from Perry and Hower (1972), appearing at 3619 m in Fig. 4b and at 3200 in Fig. 4a. Given the uncertainties inherent to the model calculations and the simplification incurred in the calculation of the K_{eq}/Ca_{eq} ratios, the similitude between Figs. 4a and b supports the validity of the models. It is interesting to note that, in Fig. 4a, the data from Awwiller (1993) and Freed and Peacor (1992), both in SE Texas, have a depression of the effective K concentration at some point between 1600 and 2800 m, followed by a large increase. As the two wells are located 11 km apart, it is very likely that these data are reflecting the real evolution of the chemical conditions in the area. The patterns in Fig. 4a of these two wells are also similar to those of the well in south central Texas (Velde and Vasseur, 1992), located within a maximum distance of ~160 km from them, in which there is a large increase of the effective K concentration in the same range of depths. This similarity may also reflect the chemistry of the porewaters. This can be true even if the age of the sediments is very different, because the chemical evolution may be caused by events that happened well

after the sedimentation and because the chemical characteristics of the sediments in one area may affect the water chemistry of the sediments in a nearby region. In this respect, it is worth noting that the highest effective K concentrations correspond to the bottom sediments from the data by Velde and Vasseur (1992) in south central Texas. These are also the oldest sediments (Table 1). It is reasonable to infer that the high K concentrations that occurred in these sediments caused also an increase in the other two wells (i.e., Freed and Peacor, 1992; Awwiller, 1993).

However, even if the relative variations of the effective K concentration mimic the K/Ca ratios from whole-rock mineral composition, the very small absolute values of K suggest that there is some other influence besides that from the competing cations. First of all, it is evident that there are intrinsic differences between the natural and experimental conditions. It is perhaps relevant to indicate here the well-known fact that mineral dissolution experiments frequently produce dissolution rates that are several orders of magnitude higher than those assessed in natural systems (White and Brantley, 1995). The reasons for this discrepancy are not known yet but it seems to be the case that certain variables are affected, suppressed or introduced in the experiments. The results from the present models probably reflect a similar situation, made more acute due to the complexity and very slow rate of illitization. There are many factors that could significantly slow down smectite illitization in shales with respect to a simple experimental system, as rock porosity, ionic strength, hydraulic conductivity and ion mobility. There are no available data on these variables from the studied sequences. However, it is evident that most of them were very different from those in the experiments by Cuadros and Linares (1996), from where the kinetic equation was derived. In my opinion, the most influential difference is ion mobility. This variable will have a great effect on the reaction kinetics because it controls the rate of supply of K and the rate of diffusion of silica and the other interlayer cations away from the clay particles. Removal of silica and interlayer cations is necessary in order to avoid local oversaturation that would stop illitization. All these species have to travel not only through the pore space between mineral grains but also in the smectite interlayer, along lattice defects or in dissolution fronts. Ion mobility in these several environments is very likely to be greatly decreased by high rock/water ratios. The smectite/water weight ratio used by Cuadros and Linares (1996) was 1/5. This ratio provides sufficient fluid to ensure a sufficiently dispersed medium, rapid ion mobility and access to and from the interlayers. This is not the case in the wells, which are rock-dominated systems and where ion mobility is much lower. The conditions in the experiments of Cuadros and Linares (1996) may have more resemblance with natural hydrothermal systems. I tried to include some of these in my models but they are more rare in the literature and I could not find any study that included all the necessary information. In conclusion, the effective K concentration in my calculations would envelop a variety of variables, most of which produce a significant decrease in the reaction rate, thus, when applying the equation derived from a water-dominated system to the field, the corresponding K concentrations appear to be much lower. However, these variables do not mask the effect of the K/Ca ratio in the rock. They affect the absolute values of the effective K concentration but the signature of the K/Ca ratio is superimposed on these values. This probably indicates that ion mobility and other variables are sufficiently homogeneous within the sequences or change sufficiently slowly with depth that they do not overprint the K/Ca signature.

The analysis of the shapes of the illitization patterns with depth shows that, where the physico-chemical conditions (effective K concentration, sedimentation rate, geothermal gradient) remain constant or nearly constant, the illitization pattern with depth is a curve shaped as a back-to-front "j." Fig. 3a shows this clearly for the simplest case, where all conditions remain constant. The other wells contain several of these steps. If illitization is slow in one of such steps, the curve becomes a straight line (first non-horizontal illitization stage in Figs. 3b, d, and e). When the illitization rate is sufficiently high, the pattern takes the shape of the characteristic convex curve that is more frequently observed. The reaction becomes so slow in the final phases that even in cases of a high geothermal gradient, a high value of available K and old sediment age, it does not proceed to completion (Fig. 3e, Table 1). This explains why the reaction is most frequently observed to stop in the range 20–10% illite layers in I–S. The results of this study are also applicable to hydrothermal systems. For example, in the sequence from California studied by Jennings and Thompson (1986) illitization was produced by an anomalously high geothermal gradient linked to crustal spreading in the East Pacific Rise. Thus, in this sequence, the sediment temperature does not necessarily increase with burial depth. Jennings and Thompson (1986) show a % smectite vs. temperature plot which has the same characteristics of the % smectite vs. depth diagrams in this work. In their case, total illitization is reached, an uncommon feature in burial illitization, because the highest temperature is 280 °C, much higher than is usual in burial diagenesis. I did not model this hydrothermal sequence because there is no information about the actual reaction time but the shape of the illitization curve and the extent of the reaction appear as totally compatible with the model. Thus, the patterns of the illitization curve observed in the field arise naturally from a kinetic equation in which the exponent of the proportion of smectite layers is high. There is no need to have recourse to different mechanisms or processes of illitization acting at different stages of the reaction progress, or producing different types of I–S layer-stacking order (*R*0, *R*1, etc.), to explain the slope changes observed in plots of % smectite vs. depth. Obviously, a high-order equation does not represent the actual mechanism of illitization. Rather, the mechanism is a complex one involving several steps and the form of the kinetic

equation is the result of the combination of all these steps. However, as indicated above, these steps and the complete process made up of them need not change during the progress of the illitization reaction. Using such a high-order equation and the most plausible data available allowed a close fit of the calculated to the experimental data in the eight sediment sequences modeled here. The only unknown input variable took values that are meaningful when contrasted with the chemical data available and when wells located in near proximity are compared. Thus, the equation and rate constants used in this work, or similar ones, are validated. Further, my results suggest that, given well-constrained I–S data and physical variables, the kinetic model can be used to gain information about the relative changes of available K within the vertical sequences and, ultimately, can be a tool to analyze K circulation within basins, provided that the variables hidden in the effective K concentration are sufficiently constant or can be assessed to a sufficient degree of accuracy.

Acknowledgments

I am grateful to S. Köhler, S. Hillier, an anonymous reviewer and E. Oelkers, the Associate Editor, for their positive criticism and suggestions.

Associate editor: Eric H. Oelkers

References

Altaner, S.P., 1989. Calculation of K diffusional rates in bentonite beds. *Geochim. Cosmochim. Acta* **53**, 923–931.

Aronson, J.L., Hower, J., 1976. Mechanism of burial metamorphism of argillaceous sediment: 2. Radiogenic argon evidence. *Geol. Soc. Am. Bull.* **87**, 738–744.

Awwiller, D.N., 1993. Illite/smectite formation and potassium mass transfer during burial diagenesis of mudrocks: a study from the Texas Gulf Coast Paleocene-Eocene. *J. Sediment. Petrol.* **63**, 501–512.

Bell, T.E., 1986. Microstructure in mixed-layer illite/smectite and its relationship to the reactions of smectite to illite. *Clay. Clay Miner.* **34**, 146–154.

Boles, J.R., Franks, S.G., 1979. Clay diagenesis in Wilcox sandstones of southwest Texas: implications of smectite diagenesis on sandstone cementation. *J. Sediment. Petrol.* **49**, 55–70.

Brown, L.F., Loucks, R.G., Treviño, R.H., Hammes, U., 2004. Understanding growth-faulted, intraslope subbasins by applying sequence-stratigraphic principles: examples from the south Texas Oligocene Frio Formation. *Am. Assoc. Petrol. Geol. Bull.* **88**, 1501–1523.

Brown, L.F., Loucks, R.G., Treviño, R., 2005. Site-specific sequence-stratigraphic section benchmark charts are key to regional chronostatigraphic systems tract analysis in growth-faulted basins. *Am. Assoc. Petrol. Geol. Bull.* **89**, 715–724.

Brownlow, A.H., 1996. Water chemistry. In: *Geochemistry*. Prentice-Hall, New Jersey.

Burst, J.F., 1969. Diagenesis of Gulf Coast clayey sediments and its possible relation to petroleum migration. *Am. Assoc. Petrol. Geol. Bull.* **53**, 73–93.

Cuadros, J., Linares, J., 1996. Experimental kinetic study of the smectite-to-illite transformation. *Geochim. Cosmochim. Acta* **60**, 439–453.

Eberl, D., Hower, J., 1976. Kinetics of illite formation. *Geol. Soc. Am. Bull.* **87**, 1326–1330.

Eberl, D.E., Whitney, G., Khoury, H., 1978. Hydrothermal reactivity of smectite. *Am. Mineral.* **63**, 401–409.

Elliott, W.C., Aronson, J.L., Matisoff, G., Gautier, D.L., 1991. Kinetics of the smectite to illite transformation in the Denver basin: clay mineral, K-Ar data, and mathematical model results. *Am. Assoc. Petrol. Geol. Bull.* **75**, 436–462.

Elliott, W.C., Edenfield, A.M., Wampler, J.M., Matisoff, G., Long, P.E., 1999. The kinetics of the smectite to illite transformation in Cretaceous bentonites, Cerro Negro, New Mexico. *Clay. Clay Miner.* **47**, 286–296.

Elliott, W.C., Matisoff, G., 1996. Evaluation of kinetic models for the smectite to illite transformation. *Clay. Clay Miner.* **44**, 77–87.

Fletcher, P., Sposito, G., 1989. The chemical modelling of clay/electrolyte interactions for montmorillonite. *Clay Miner.* **24**, 375–391.

Freed, R.L., Peacor, D.R., 1992. Diagenesis and the formation of authigenic illite-rich I/S crystals in Gulf Coast shales: TEM study of clay separates. *J. Sediment. Petrol.* **62**, 220–234.

Galloway, W.E., 1990. Paleogene depositional episodes, genetic stratigraphic sequences, and sediment accumulation rates NW Gulf of Mexico basin. In: *GCSSEPM Foundation 11th Annual Research Conference*. Program and abstracts, pp. 165–176.

Galloway, W.E., Williams, T.A., 1991. Sediment accumulation rates in time and space: paleogene genetic stratigraphic sequences of the northwestern Gulf of Mexico basin. *Geology* **19**, 986–989.

Hillier, S., Mátyás, J., Matter, A., Vasseur, G., 1995. Illite/smectite diagenesis and its variable correlation with vitrinite reflectance in the Pannonian Basin. *Clay. Clay Miner.* **43**, 174–183.

Howard, J.J., Roy, D.M., 1985. Development of layer charge and kinetics of experimental smectite alteration. *Clay. Clay Miner.* **33**, 81–88.

Hower, J., Eslinger, E.V., Hower, M.E., Perry, E.A., 1976. Mechanism of burial metamorphism of argillaceous sediment: 1. Mineralogical and chemical evidence. *Geol. Soc. Am. Bull.* **87**, 725–737.

Huang, W., Longo, J., Pevear, D., 1993. An experimentally derived kinetic model for smectite-to-illite conversion and its use as a geothermometer. *Clay. Clay Miner.* **41**, 162–177.

Inoue, A., Utada, M., Wakita, K., 1992. Smectite-to-illite conversion in natural hydrothermal systems. *Appl. Clay Sci.* **7**, 131–145.

Jennings, S., Thompson, G.R., 1986. Diagenesis of Plio-Pleistocene sediments of the Colorado River Delta, southern California. *J. Sediment. Petrol.* **56**, 89–98.

Langmuir, D., 1997. General controls on natural water chemistry. In: *Aqueous Environmental Geochemistry*. Prentice-Hall, New Jersey.

Masuda, H., O'Neil, J.R., Jiang, W.-T., Peacor, D.R., 1996. Relation between interlayer composition of authigenic smectite, mineral assemblages, I/S reaction rate and fluid composition in silicic ash of the Nankai trough. *Clay. Clay Miner.* **44**, 443–459.

Meunier, A., Lanson, B., Velde, B., 2004. Composition variation of illite-vermiculite-smectite mixed-layer minerals in a bentonite bed from Charente (France). *Clay Miner.* **39**, 317–332.

Mosser-Ruck, R., Cathelineau, M., Baronnet, A., Trouiller, A., 1999. Hydrothermal reactivity of K-smectite at 300 °C and 100 bar: dissolution-crystallization process and non-expandable dehydration smectite formation. *Clay Miner.* **34**, 275–290.

Mosser-Ruck, R., Devineau, K., Charpentier, D., Cathelineau, M., 2005. Effects of ethylene glycol saturation protocols on XRD patterns: a critical review and discussion. *Clay. Clay Miner.* **53**, 631–638.

Murray, G.E., 1960. Geologic framework of Gulf coastal province of United States. In: Shepard, F.P., Phleger, F.P., van Andel, T.J. (Eds.), *Recent Sediments, Northwest Gulf of Mexico*. The American Association of Petroleum Geologists, Tulsa, OK, pp. 5–33.

Perry, E., Hower, J., 1970. Burial diagenesis in Gulf Coast pelitic sediments. *Clay. Clay Miner.* **18**, 165–177.

Perry, E.A., Hower, J., 1972. Late-stage dehydration in deeply buried pelitic sediments. *Am. Assoc. Petrol. Geol. Bull.* **56**, 2013–2021.

Pytte, A.M., Reynolds, R.C., 1989. The thermal transformation of smectite to illite. In: Naeser, N.D., McCulloh, T.H. (Eds.), *The Thermal History of Sedimentary Basins*. Springer, New York, pp. 133–140.

Roaldset, E., Wei, W., Grimstad, S., 1998. Smectite to illite conversion by hydrous pyrolysis. *Clay Miner.* **33**, 147–158.

Roberson, H.E., Lahann, R.W., 1981. Smectite to illite conversion rates: effects of solution chemistry. *Clay. Clay Miner.* **29**, 129–135.

Velde, B., Ijima, A., 1988. Comparison of clay and zeolite mineral occurrences in Neogene age sediments from several deep wells. *Clay. Clay Miner.* **36**, 337–342.

Velde, B., Vasseur, G., 1992. Estimation of the diagenetic smectite to illite transformation in time–temperature space. *Am. Mineral.* **77**, 967–976.

Verburg, K., Baveye, P., 1996. Cation exchange hysteresis scanning curves: mathematical description and interpretation. *Eur. J. Soil Sci.* **47**, 345–356.

White, A.F., Brantley, S.L., 1995. In: *Chemical Weathering Rates of Silicate Minerals. Reviews in Mineralogy*, vol. 31. Mineralogical Society of America, 583 pp.

Whitney, G., Northrop, H.R., 1988. Experimental investigation of the smectite to illite reaction: Dual reaction mechanisms and oxygen-isotope systematics. *Am. Mineral.* **73**, 77–90.

Ye, Q., Matthews, R.K., Galloway, W.E., Frohlich, C., Gan, S., 1993. High-frequency glacioeustatic cyclicity in the early Miocene and its influence on coastal and shelf depositional systems, NW Gulf of Mexico basin. In: *GCSSEPM Foundation 14th Annual Research Conference. Rates of Geological Processes*. Program and abstracts, pp. 287–298.